

Further Evidence for Threefold Maximal Lepton Mixing and a Hierarchical Spectrum of Neutrino Mass-Squared Differences

P. F. Harrison

Physics Department, Queen Mary and Westfield College
Mile End Rd. London E1 4NS. UK ¹

and

D. H. Perkins

Nuclear Physics Laboratory, University of Oxford
Keble Road, Oxford OX1 3RH. UK ²

and

W. G. Scott

Rutherford Appleton Laboratory
Chilton, Didcot, Oxon OX11 0QX. UK ³

Abstract

The phenomenological case for threefold maximal lepton mixing is strengthened by more detailed comparison with existing data. The atmospheric neutrino data are self-consistent and in good agreement with the threefold maximal mixing prediction $R = 2/3$ ($\chi^2/\text{DOF} = 4.3/5$, CL = 51%). Including partially-contained event data, the zenith angle dependence also points to threefold maximal mixing, ruling out a range of mixing schemes, including that of Fritzsch and Xing. Accounting for *de facto* uncertainties in solar neutrino fluxes, the solar neutrino data (including HOMESTAKE) are shown to be consistent with threefold maximal mixing ($\chi^2/\text{DOF} = 5.1/3$, CL = 16%), as is the upper limit from the LSND appearance experiment. Detailed predictions for forthcoming long-base-line reactor and accelerator experiments are presented.

To be published in Physics Letters B

¹E-mail:p.f.harrison@qmw.ac.uk

²E-mail:d.perkins1@physics.oxford.ac.uk

³E-mail:w.g.scott@rl.ac.uk

1. INTRODUCTION

The notion of maximal lepton mixing [1] and threefold maximal lepton mixing in particular [2] is currently exciting renewed interest [3] [4]. In the case of threefold maximal mixing the mixing matrix may be written:

$$\begin{array}{c} \nu_1 \\ \nu_2 \\ \nu_3 \end{array} \begin{pmatrix} \nu_e & \nu_\mu & \nu_\tau \\ \omega/\sqrt{3} & \omega^2/\sqrt{3} & 1/\sqrt{3} \\ \omega^2/\sqrt{3} & \omega/\sqrt{3} & 1/\sqrt{3} \\ 1/\sqrt{3} & 1/\sqrt{3} & 1/\sqrt{3} \end{pmatrix} \quad (1)$$

with ν_1 , ν_2 and ν_3 the neutrino mass eigenstates, ν_e , ν_μ and ν_τ the neutrino flavour eigenstates, and ω a complex cube-root of unity.

In Ref. [3] we outlined the phenomenology of neutrino oscillations in a threefold maximal mixing scenario with a hierarchical neutrino mass spectrum, which may explain the atmospheric [5] [6] [7] [8] [9] and solar [10] [11] [12] [13] neutrino deficits (the scenario discussed by Giunti et al. [4] is closely related to ours but differs in detail regarding the light neutrino masses). The key feature is that, independent of the initial neutrino flavour l ($l = e, \mu, \tau$) the flavour survival probability $P(l \rightarrow l)$, averaged over neutrino energies, is equal to $5/9$, over an extremely wide range of L/E values (L is the propagation length and E is the neutrino energy). This range extends from $L/E \simeq 10^2$ m/MeV, based on the terrestrial data (mainly the atmospheric results, but including the reactor and accelerator data) to $L/E \gtrsim 10^{12}$ m/MeV, based on the solar data. The corresponding appearance probability $P(l \rightarrow l')$ to produce a neutrino of a different flavour l' ($l' \neq l$) is equal to $2/9$ independent of the initial and final neutrino flavours, over the same L/E range. The particular numerical ratios $5/9$ and $2/9$ reflect the democracy of couplings intrinsic to threefold maximal mixing (Eq. 1). The wide range in L/E over which the measured probabilities remain at these values is the experimental signature of a hierarchical spectrum of mass-squared differences for the neutrinos.

Of course, at sufficiently small L/E values $P(l \rightarrow l) = 1$, consistent with ordinary lepton flavour conservation. As detailed in Ref. [3] an abrupt ‘threshold’ in L/E marks the transition from $P(l \rightarrow l) = 1$ to $P(l \rightarrow l) = 5/9$. It is the location of this threshold on the L/E scale ($L/E \simeq 10^2$ m/MeV) which fixes the largest neutrino mass-squared difference $\Delta m^2 \simeq (0.72 \pm 0.18) \times 10^{-2}$ eV². If none of the three neutrino mass eigenstates are degenerate then $P(l \rightarrow l) = 1/3$ asymptotically, and there will be a second threshold at some larger L/E value, marking the descent from $P(l \rightarrow l) = 5/9$ to $P(l \rightarrow l) = 1/3$. The second threshold (if it exists) fixes the smaller neutrino mass-squared difference $\Delta m'^2$. We found no convincing evidence for a second threshold over the L/E range up to and including the solar data and placed the limit

$\Delta m^2 < 0.90 \times 10^{-11} \text{ eV}^2$ at 90% confidence (based essentially on the data from the two gallium experiments [12] [13]). The above results establish that the spectrum of mass-squared differences for the neutrinos is hierarchical ($\Delta m'^2 \ll \Delta m^2$). On the assumption that the neutrino masses themselves exhibit a hierarchical spectrum (like that of the charged leptons and quarks) they may be re-expressed in terms of the neutrino masses ($m_1 < m_2 < m_3$) as follows: $m_3 \simeq 85 \pm 10 \text{ meV}$, $m_1, m_2 < 3 \text{ } \mu\text{eV}$ at 90% confidence (see Ref. [3] for details of fits).

On the basis of the above mass spectrum, the neutrinos are too light to be considered useful hot dark matter candidates [14]. The mass of the heavy neutrino ν_3 is consistent with a ‘see-saw’ formula [15] relating the masses of the neutrinos to the masses of the up-type quarks, for a heavy (right-handed) majorana mass $M_R \simeq 3.6 \times 10^{14} \text{ GeV}$ (a see-saw relation involving the charged lepton masses would yield a smaller value of M_R , by a factor of 10^4). The above results for the neutrino masses may also be quoted in terms of the corresponding compton wavelengths, viz. $\lambda_3 \simeq 15 \text{ } \mu\text{m}$, $\lambda_1, \lambda_2 > 40 \text{ cm}$.

The apparent degeneracy or near-degeneracy of the two light neutrinos ν_1 and ν_2 makes further progress very difficult. As long as ν_1 and ν_2 remain effectively degenerate, only the couplings of the heavy neutrino ν_3 are probed and not those of ν_1 and ν_2 separately. Hitherto unproposed *ad hoc* mixing schemes in which the ν_3 is maximally-mixed (ie. has ν_e, ν_μ, ν_τ content $1/3, 1/3, 1/3$) but which are otherwise arbitrary have identical phenomenology to threefold maximal mixing over the L/E range explored in the atmospheric and solar neutrino experiments. The complete set of such schemes is readily generated starting from the threefold maximal mixing matrix (Eq. 1) by forming linear combinations of the first two rows, with arbitrary complex coefficients ($c_\theta e^{i\phi}, -s_\theta e^{-i\phi}$) and ($s_\theta e^{i\phi}, c_\theta e^{-i\phi}$) for ν_1 and ν_2 respectively:

$$\begin{array}{c} \nu_e \\ \nu_\mu \\ \nu_\tau \end{array} \begin{array}{ccc} \nu_e & \nu_\mu & \nu_\tau \\ \left(\begin{array}{ccc} (c_\theta e^{i\phi} \omega - s_\theta e^{-i\phi} \omega^2)/\sqrt{3} & (c_\theta e^{i\phi} \omega^2 - s_\theta e^{-i\phi} \omega)/\sqrt{3} & (c_\theta e^{i\phi} - s_\theta e^{-i\phi})/\sqrt{3} \\ (s_\theta e^{i\phi} \omega^2 + c_\theta e^{-i\phi} \omega)/\sqrt{3} & (s_\theta e^{i\phi} \omega + c_\theta e^{-i\phi} \omega^2)/\sqrt{3} & (s_\theta e^{i\phi} + c_\theta e^{-i\phi})/\sqrt{3} \\ 1/\sqrt{3} & 1/\sqrt{3} & 1/\sqrt{3} \end{array} \right) & (2) \end{array}$$

where $c_\theta = \cos \theta$ and $s_\theta = \sin \theta$. Threefold maximal mixing predicts $\theta = 0 \pmod{\pi/2}$ with ϕ a redundant phase. More generally θ and ϕ are both measurable. Data on neutrinos from supernovae ($L/E \gtrsim 10^{20} \text{ m/MeV}$) although presently too sparse to yield reliable information on mixing [16] might eventually measure the couplings of the light neutrinos and test the above prediction. If ν_1 and ν_2 are truly degenerate (as is not excluded by the present data) then all such mixing schemes are equivalent and the mixing may then be defined to be threefold maximal by choice.

On the other hand, proposed mixing schemes in which one (and only one) of the neutrino *flavour* eigenstates is maximally-mixed (ie. has ν_1, ν_2, ν_3 content $1/3, 1/3,$

1/3) can in general be distinguished by the data in the L/E range currently accessed (so that it matters whether the postulated maximally-mixed state constitutes a ‘row’ or ‘column’ of the mixing-matrix). The complete set of real mixing-matrices with the ν_e maximally-mixed has been discussed by Acker et al. [17], while a particular (real) mixing-matrix with the ν_τ maximally-mixed is singled out in a recent paper by Fritzsche and Xing [18]. The complete set of mixing matrices with the ν_τ maximally mixed for example (as in the Fritzsche-Xing ansatz) is readily generated analogously to Eq. 2:

$$\begin{array}{c} \nu_e \\ \nu_\mu \\ \nu_\tau \end{array} \left(\begin{array}{ccc} (c_\theta e^{i\phi}\omega - s_\theta e^{-i\phi}\omega^2)/\sqrt{3} & (c_\theta e^{i\phi}\omega^2 + s_\theta e^{-i\phi}\omega)/\sqrt{3} & 1/\sqrt{3} \\ (c_\theta e^{i\phi}\omega^2 - s_\theta e^{-i\phi}\omega)/\sqrt{3} & (c_\theta e^{i\phi}\omega + s_\theta e^{-i\phi}\omega^2)/\sqrt{3} & 1/\sqrt{3} \\ (c_\theta e^{i\phi} - s_\theta e^{-i\phi})/\sqrt{3} & (c_\theta e^{i\phi} + s_\theta e^{-i\phi})/\sqrt{3} & 1/\sqrt{3} \end{array} \right) \quad (3)$$

where the Fritzsche-Xing ansatz is reproduced in the case $\theta = \pi/4$ with $\phi = 0$. While such schemes are also fairly described as *ad hoc* they do yield valid candidate mixing matrices which can be tested against experiment (see Section 2 and Section 3 below).

It is hardly necessary to emphasise here that the notion of large mixing in the lepton sector is by no means a universal tenet. On the contrary, the widely accepted MSW solution [19] [20] [21] to the solar neutrino problem currently favours small mixing angles in the lepton sector, as do recent results from the LSND [33] appearance experiment (see Section 3 and Section 4 below).

In this paper we re-examine the experimental evidence for (and against) threefold maximal lepton mixing, in comparison with a range of more general mixing schemes. Detailed predictions for forthcoming reactor and accelerator experiments are given, based on the threefold maximal mixing scenario.

2. THE ATMOSPHERIC DATA

The best measured quantity in the atmospheric neutrino experiments is the atmospheric neutrino ratio $R = (\mu/e)_{DATA}/(\mu/e)_{MC}$, where $(\mu/e)_{DATA}$ is the measured ratio of muon to electron events, and $(\mu/e)_{MC}$ is the expected ratio of muon to electron events, assuming no oscillations. Results for R for fully contained events from the various underground experiments are summarised in Table 1. The KAMIOKA and IMB experiments are based on the water-Cerenkov technique, while FREJUS, NUSEX and SOUDAN are ionisation-based tracking detectors. A common $\pm 5\%$ uncertainty in the predicted flux ratio has been subtracted from the quoted systematic errors where appropriate, so that the errors given here should be largely independent experiment-to-experiment. The same data are plotted in Figure 1, where the errors shown combine the above statistical and systematic errors in quadrature.

Contrary to what has been asserted (eg. Ref. [22]), there is no evidence for a discrepancy between the results of the water-Cerenkov and tracking detectors, at least

for the contained event data. A weighted mean over the five experiments gives $R = 0.64 \pm 0.06$ ($\chi^2/\text{DOF} = 4.2/4$, CL = 38%). In the threefold maximal mixing scenario one expects $R = 2/3$ [3] for contained events, in the approximation that the flux ratio at production $F = \phi(\nu_\mu + \bar{\nu}_\mu)/\phi(\nu_e + \bar{\nu}_e)$ ($\equiv \nu_\mu/\nu_e$) is equal to 2/1 at low energy. In Figure 1 the broken line shows the threefold maximal mixing prediction $R = 2/3$. The contained event data are clearly consistent with this ($\chi^2/\text{DOF} = 4.3/5$, CL = 51%), the higher confidence level for the maximal mixing hypothesis reflecting the reduction in the number of fitted parameters. Furthermore, in the threefold maximal mixing scenario, the final ν_e rate turns out to be unaffected by the oscillations (in the approximation $\nu_\mu/\nu_e = 2/1$), so that it is the ν_μ rate which is expected to be reduced by a factor of 2/3, which is also in agreement with observation [23] for the ν_μ and ν_e rates separately.

The KAMIOKA partially-contained sample (the so-called ‘multi-GeV’ data-set) provides a measurement of the zenith angle dependence of R and hence the L/E dependence. Although there is no evidence for neutrino oscillations in the atmospheric data for $L/E < 10^2$ m/MeV, the data with $L/E > 10^2$ m/MeV can be utilised to yield independent information on survival *and* appearance probabilities, exploiting the dependence of the initial ν_μ/ν_e flux ratio on energy and zenith angle. Figure 2a shows the measured value of the atmospheric neutrino ratio R plotted versus the initial flux ratio F for all the data with $L/E > 10^2$ m/MeV. The point plotted at $F = 2.2$ is the overall average of the contained event data, discussed above. The points at larger values of F are based on the KAMIOKA partially-contained (multi-GeV) data-set. The value of F for each point was calculated (as a function of energy and zenith angle) using a Monte Carlo simulation of the propagation and decay of pions and muons in the atmosphere.

In the presence of neutrino oscillations the predicted value of R as a function of F is given by: $R = (P(e \rightarrow \mu) + F \times P(\mu \rightarrow \mu))/(F \times P(e \rightarrow e) + F^2 \times P(\mu \rightarrow e))$. In the maximal mixing scenario $P(\mu \rightarrow \mu) = P(e \rightarrow e) = 5/9$ and $P(e \rightarrow \mu) = P(\mu \rightarrow e) = 2/9$ leading to the dependence shown by the dashed curve in Figure 2a, which is clearly consistent with the data ($\chi^2/\text{DOF} = 1.2/2$, CL = 55%). In the Fritzsche-Xing model (see Section 1) [18], $P(\mu \rightarrow \mu) = 5/9$ but $P(e \rightarrow e) = 1$ and $P(\mu \rightarrow e) = P(e \rightarrow \mu) = 0$ for the atmospheric data, so that $R = 5/9$ independent of F as shown by the dotted line. The data rule out the Fritzsche-Xing model with better than 99% confidence ($\chi^2/\text{DOF} = 9.4/2$, CL = 0.7%).

The full range of mixing schemes with the ν_τ maximally mixed (Eq. 3) may also be tested against experiment using the data of Figure 2a. All these schemes are as well motivated a priori as the Fritzsche-Xing model itself. It turns out that in the L/E range between the two thresholds, ie. for $(\Delta m^2/2)^{-1} \lesssim L/E \lesssim (\Delta m'^2/2)^{-1}$, observables

depend only on the product $\sin 2\theta \cos 2\phi$. Specifically $P(\mu \rightarrow \mu) = 1/2 + 2/9(1/2 - \sin 2\theta \cos 2\phi)^2$, $P(e \rightarrow e) = 1/2 + 2/9(1/2 + \sin 2\theta \cos 2\phi)^2$ and $P(e \rightarrow \mu) = P(\mu \rightarrow e) = 2/9(1 - \sin^2 2\theta \cos^2 2\phi)$. Beyond the second threshold ($L/E \gtrsim (\Delta m'^2/2)^{-1}$) if present, $P(\mu \rightarrow \mu) = P(e \rightarrow e) = 1/3(1 + 1/2 \sin^2 2\theta)$ and $P(\mu \rightarrow e) = P(e \rightarrow \mu) = 1/3(1 - 1/2 \sin^2 2\theta)$. Remaining probabilities (involving the τ) follow immediately in each case, since the rows and columns of the probability matrices sum to unity.

On the assumption that the neutrino mass spectrum is hierarchical ($\Delta m'^2 \ll \Delta m^2$) the formulae valid between the two thresholds apply. The calculated χ^2 is plotted as a function of $\sin 2\theta \cos 2\phi$ in Figure 2b. Threefold maximal mixing predicts $\sin 2\theta \cos 2\phi = 0$, while the Fritzsche-Xing model corresponds to $\sin 2\theta \cos 2\phi = 1$. The best fit yields $\sin 2\theta \cos 2\phi = 0.07 \pm \begin{smallmatrix} 0.28 \\ 0.15 \end{smallmatrix}$. Thus most of these schemes are ruled out by the data, along with the Fritzsche-Xing model, while threefold maximal mixing is both fully consistent with the data and very close to the preferred solution.

3. THE SOLAR DATA

Any analysis of the existing solar data requiring a knowledge of the solar neutrino fluxes, relies on predictions from solar models. In Figure 3, the Standard Solar Model predictions of Proffitt (PR) [24], Bahcall and Pinsonneault (BP) [25], Turk-Chiese and Lopes (TL) [26], and Dar and Shaviv (DS) [27] are compared side-by-side, by plotting the ratio of observed to predicted rates in each of the four solar neutrino experiments, KAMIOKA [10], HOMESTAKE [11], SAGE [12] and GALLEX [13]. The KAMIOKA and HOMESTAKE experiments are primarily sensitive to ^8B neutrinos, and the resulting suppression factors are seen to be strongly dependent on the flux calculation used. On the other hand, in the two gallium experiments, SAGE [12] and GALLEX [13], the main contribution to the rate is from pp neutrinos, and the corresponding dependence is seen to be small. Furthermore, the efficiency of both the SAGE and GALLEX detectors has been measured (to $\sim 10\%$ accuracy) using a laboratory neutrino source (^{51}Cr).

In view of the particular stability and reliability of the gallium data, a number of conclusions follow immediately. In Figure 3 the dashed line $P(e \rightarrow e) = 5/9$ is the threefold maximal mixing prediction applying in the case that the second threshold is taken to lie beyond the solar data in L/E , as is assumed in Ref. [3]. It is clear that the results from the two gallium experiments are in excellent agreement with this. The mean of the SAGE and GALLEX results averaged over the four flux models yields $P(e \rightarrow e) = 0.55 \pm 0.05$, to be compared with the $5/9$ expected. The scenario inferred by Giunti et al. [4] with the second threshold coinciding in L/E with the solar data (leading to $\Delta m'^2 \simeq 10^{-10} \text{ eV}^2$ [4]) does not now seem well-founded, and in the same way the scenario described by Acker et al. [17] (see Section 1) which places all the solar

data beyond the second threshold ($\Delta m'^2 \simeq \Delta m^2 \simeq 10^{-2} \text{ eV}^2$ [17]) is also now excluded by the gallium data (both Giunti et al. and Acker et al. would predict $P(e \rightarrow e) \simeq 1/3$ in the gallium experiments).

It should be added that we have not analysed the complete set of models with the ν_e maximally mixed, as in the model of Acker et al. The relevant formulae follow immediately from those given for ν_τ maximal mixing, under the interchange $e \leftrightarrow \tau$. It may be remarked that putting $\theta = \pi/4$ then yields the set of real mixing matrices discussed by Acker et al. and that putting $\phi = \pi/12$ (in addition) gives a real matrix with the ν_3 (as well as the ν_e) maximally mixed. This is *one* of the infinite set of matrices (Eq. 2) which reproduce the phenomenology of threefold maximal mixing up to the second threshold which were discussed in Section 1. We do not consider this particular example to be of any special interest.

Coming now to the KAMIOKA and HOMESTAKE results, we previously concluded [3] that the KAMIOKA point was consistent with $P(e \rightarrow e) = 5/9$ and that the HOMESTAKE point was low, relying on an average of the BP and TL flux calculations. From Figure 3 it is apparent that, if one uses the DS fluxes, it is the HOMESTAKE point which is consistent with 5/9, and the KAMIOKA point which is high. That such large differences should exist between the different flux calculations, is clearly very unsatisfactory. The predicted ${}^8\text{B}$ flux varies by more than a factor of two between the most extreme models, which is far outside the error limits quoted by the authors of the individual calculations, with no indication of an emerging consensus in the literature. Under the circumstances, it would seem prudent [28] to avoid drawing conclusions which depend on the predicted ${}^8\text{B}$ flux, if at all possible.

New results are presented here, obtained by refitting the existing solar data taking the ${}^8\text{B}$ flux as an adjustable parameter. In so far as they are known, correlations between the ${}^8\text{B}$ flux and the other flux components are taken into account in these fits by linearly interpolating the other flux components, between the above four flux calculations, as a function of the ${}^8\text{B}$ flux. In addition to the threefold maximal mixing solution, all of the well-known 2×2 solutions to the solar neutrino problem, viz. small-angle MSW, large-angle MSW and the ‘just-so’ vacuum oscillation solution [29], are found to survive as distinct χ^2 minima in these fits (matter effects, essentially inoperative in the case of maximal mixing [3], are incorporated where needed here using standard 2×2 formulae [30]). Best-fit parameters and confidence levels are of course modified, with respect to those usually quoted, in most cases.

The results of these fits are plotted in Figure 4, as a function of L/E [3]. Figure 4a shows the threefold maximal mixing fit, which assumes $P(e \rightarrow e) = 5/9$ independent of energy. Further details of this fit are given in Table 2. The best-fit value for the total ${}^8\text{B}$ flux is $\Phi({}^8\text{B}) = 3.4 \times 10^6 \text{ cm}^2 \text{ s}^{-1}$ ($\chi^2/\text{DOF} = 5.1/3$, CL = 16%), which

lies between the TL and DS predictions. Figure 4b shows the small angle MSW fit, which gives $\Phi(^8\text{B}) = 4.4 \times 10^6 \text{ cm}^2 \text{ s}^{-1}$ (essentially the TL prediction), with $\sin \theta = 0.030$, $\Delta m^2 = 0.61 \times 10^{-5} \text{ eV}^2$ ($\chi^2/\text{DOF} = 0.004/1$, CL = 96%). For the large angle MSW and ‘just-so’ vacuum oscillation solutions, the best-fit ^8B flux turns out to be larger/smaller than the most extreme model in each case, viz. the PR and DS models respectively. To avoid relying on extrapolated fluxes, the results for the large angle MSW fit (Figure 4c) are given using the PR flux, viz. $\Phi(^8\text{B}) = 6.5 \times 10^6 \text{ cm}^2 \text{ s}^{-1}$, $\sin \theta = 0.50$, $\Delta m^2 = 2.1 \times 10^{-5} \text{ eV}^2$ ($\chi^2/\text{DOF} = 1.8/2$, CL = 41%). Similarly for the ‘just-so’ vacuum oscillation fit (Figure 4d) the DS flux is used, viz. $\Phi(^8\text{B}) = 2.8 \times 10^6 \text{ cm}^2 \text{ s}^{-1}$, $\sin \theta = 0.71$, $\Delta m^2 = 1.8 \times 10^{-10} \text{ eV}^2$ ($\chi^2/\text{DOF} = 2.2/2$, CL = 34%). In each of Figures 4a-d the data points are plotted using the above flux values, with a correction [3] applied to the KAMIOKA point to account for the neutral-current contribution. The solid curve in each case is the expected suppression as a function of L/E , corresponding to the fitted mixing parameters.

As is well-known, the MSW effect is observable only over a limited range in parameter space, corresponding to about four orders of magnitude in neutrino mass-squared difference (or two orders of magnitude in terms of neutrino mass). In Figures 4b-4d the broken curves show the effect of rescaling the relevant neutrino mass by a factor 100 (up or down) with respect to the best-fit value, keeping the mixing angle fixed. The expectations are scaled, or translated on the logarithmic L/E -scale, proportional (to the square of) the mass rescaling. The range of observability of the MSW effect is determined by the maximum width of the ‘bathtub’ (attained in the case of the large angle solution). Similarly for the vacuum oscillation solution, with the solar data spanning less than two orders of magnitude on the L/E scale, the associated threshold is observable only if the neutrino mass-squared difference is ‘just-so’. While an element of ‘fine-tuning’ undoubtedly enters therefore, for both the MSW and vacuum oscillation solutions (which is not present in the case of threefold maximal mixing), it is difficult to know how to take this into account quantitatively. The conclusions which follow are based simply on the straightforward confidence levels quoted above.

Based on the above confidence levels, the small angle MSW fit continues to give the best account of the solar data, with both the large angle MSW and ‘just-so’ vacuum oscillation solutions also having higher fit-probabilities than threefold maximal mixing, albeit by somewhat smaller factors. On the other hand, threefold maximal mixing is *not* excluded by the solar data (including the HOMESTAKE point) even at 90% confidence. A clear prediction of the threefold maximal mixing scenario, independent of the predicted ^8B flux, is that the KAMIOKA and HOMESTAKE experiments must ultimately measure the same suppression. Presumably future solar experiments, in particular SNO [31], will eventually settle the question of the ^8B flux. Meanwhile,

data from the new KAMIOKA detector (SUPER-K [32]) will obviously be of very considerable interest.

4. ACCELERATOR AND REACTOR EXPERIMENTS

The LSND [33] collaboration claim a positive signal for $\bar{\nu}_\mu \rightarrow \bar{\nu}_e$ in an appearance experiment ($L/E \simeq 0.98$ m/MeV), with an appearance probability $P(\bar{\mu} \rightarrow \bar{e}) \simeq (0.31 \pm 0.10 \pm 0.05)\%$. The LSND result is plotted in Figure 5, together with the upper limits given by KARMEN [35] ($L/E \simeq 0.44$ m/MeV) and BNL-776 [36] ($L/E \simeq 0.71$ km/GeV). The curve shows the predicted appearance probability in threefold maximal mixing, plotted as a function of L/E , assuming $\Delta m^2 \simeq 0.72 \times 10^{-2}$ eV² [3]. Taken at face value, the LSND result would immediately exclude threefold maximal mixing (at least with $\Delta m^2 \simeq 0.72 \times 10^{-2}$ eV²). Of course, the LSND result can be accommodated together with the atmospheric and solar results in a more general mixing scheme [37]. It should be pointed out, however, that the LSND result is only marginally consistent with the upper limits from KARMEN and BNL-776, and that, furthermore, due to unexplained anomalies in the spatial distribution of the events in the detector, the LSND result remains controversial, even within the LSND collaboration. The upper limit obtained by Hill [34] from a subset of the LSND data is also plotted in Figure 5 and is clearly fully consistent with threefold maximal mixing.

In Figure 5, the expected sensitivities of the two CERN appearance experiments, CHORUS [38] and NOMAD [39] ($L/E \simeq 0.05$ km/GeV) are also indicated (90% confidence upper limits are shown, based on the projected running). In the threefold maximal mixing scenario the predicted appearance rates at these L/E values are extremely small ($P(\mu \rightarrow \tau) \simeq 10^{-7}$). If threefold maximal mixing is correct, no tau-lepton events should be seen in either of these experiments.

Assuming threefold maximal mixing is correct, spectacular effects are expected in long-baseline reactor and accelerator experiments, planned or in progress. Results on $\bar{\nu}_e$ survival rates from the CHOOZ [40] reactor experiment ($L/E \simeq 200$ m/MeV) are expected within months, and from the PALO-VERDE [41] reactor experiment ($L/E \simeq 150$ m/MeV) within one year. The MINOS [42] experiment ($L/E \simeq 50$ km/GeV) will utilise a ν_μ beam produced by the FNAL main-injector in conjunction with a new detector located in the SOUDAN mine, and is expected to be operational by the year 2001. MINOS should be sensitive to ν_e and ν_τ appearance as well as ν_μ disappearance. Similar long-baseline accelerator experiments, planned or proposed, include KEK/KAMIOKA [43] and CERN/GRAN-SASSO [44]. In Figure 6 the threefold maximal mixing predictions for the CHOOZ, PALO-VERDE and MINOS experiments are plotted out in full (experimental resolution effects are not included in these plots, but are not expected to dominate). With both L and E relatively well determined,

each of these experiments should succeed in mapping out essentially one full oscillation cycle, providing the first detailed and definitive proof of the existence of neutrino flavour oscillations.

5. CONCLUSION

Having re-examined the available experimental evidence, the threefold maximal mixing scenario remains our preferred solution to the problem of lepton mixing. It provides a good fit *ab initio* to 26 data points from 19 out of 20 disappearance experiments [3]. As discussed in this paper, the discrepancy with HOMESTAKE may now be reconciled. Regarding the appearance data, only the LSND result is in disagreement with threefold maximal mixing.

While the suppression factors measured in the atmospheric and solar experiments are naturally interpreted in terms of neutrino oscillations (consistent with the threefold maximal mixing scenario) definitive and detailed proof of the existence of actual neutrino oscillations can only come from laboratory experiments with controllable man-made beams, and precision detectors. Forthcoming long-baseline projects at reactors and accelerators should, therefore, be decisive.

In the longer term, attention will perhaps turn to the second threshold and the measurement of Δm^2 , where, as regards the couplings of the two light neutrinos, experiments sensitive to neutrinos from distant supernovae [45] may well be our only hope of progress.

Aknowledgement

We are indebted to J. N. Bahcall, A. Dar, Y. Declais, P. I. Krastev, S. T. Petcov and S. Sarkar for helpful correspondence relating to the topics discussed in this paper.

References

- [1] V. Gribov and B. Pontecorvo. Phys. Lett. 28B (1969) 493.
S. Nussinov. Phys. Lett. B 63 (1976) 201.
R. Foot, H. Lew and R. R. Volkas. Mod. Phys. Lett. A7 (1992) 2567.
- [2] L. Wolfenstein. Phys. Rev. D18 (1978) 958.
N. Cabibbo. Phys. Lett. B 72 (1978) 333.
P. F. Harrison and W. G. Scott. Phys. Lett. B 333 (1994) 471.
- [3] P. F. Harrison, D. H. Perkins and W. G. Scott.
Phys. Lett. B 349 (1995) 137; B374 (1996) 111.
- [4] C. Giunti, C. W. Kim and J. D. Kim. Phys. Lett. B 352 (1995) 357.
S. M. Bilenky, C. Giunti and C. W. Kim. Phys. Lett. B 380 (1996) 331.
- [5] K. S. Hirata et al. Phys. Lett. B 205 (1988) 416; B280 (1992) 146.
Y. Fukada et al. Phys. Lett. B335 (1994) 237.
- [6] R. Becky-Szandy et al. Phys. Rev. D46 (1992) 3720.
D. Casper et al. Phys. Rev. Lett. 66 (1992) 2561.
- [7] C. Berger et al. Phys. Lett B 227 (1989) 489; B 245 (1990) 305.
- [8] M. Aglietta et al. Europhys. Lett. 15 (1991) 559.
- [9] W. W. M. Allison et al. Phys. Lett. B391 (1997) 491.
RAL preprint RAL-P-96-007.
- [10] K.S. Hirata et al. Phys. Rev. Lett. 65 (1990) 1297; 66 (1991) 9.
Phys. Rev. D44 (1992) 146.
- [11] B. T. Cleveland et al. Nucl. Phys. B (Proc. Suppl.) 38 (1995) 47.
- [12] A. I. Abazov et al. Phys. Rev. Lett. 67 (1991) 3332.
J. N. Abdurashitov et al. Phys. Lett. B328 (1994) 234.
Phys. Rev. Lett. 77 (1996) 4708.
- [13] P. Anselmann et al. Phys. Lett. B 285 (1992) 376; B 314 (1993) 445;
B342 (1995) 440; B357 (1995) 237.
W. Hampel et al. Phys. Lett. B 388 (1996) 384.
- [14] Q. Shafi and F. W. Stecker Phys. Rev. Lett. 53 (1984) 1292.
D. O. Caldwell and R. N. Mohapatra Phys. Rev. D48 (1993) 3259.

- [15] M. Gell-Mann, P. Ramond and R. Slansky. Supergravity. ed. P. van Nieuwenhuizen and D. Z. Freedman, North-Holland (1979).
T. Yanagida. Workshop on Unified Theory and Baryon Number in the Universe. Tsukuba (1979).
- [16] L. M. Krauss et al. Nucl. Phys. B437 (1995) 243.
- [17] A. Acker et al. Phys. Lett. B 298 (1993) 149.
- [18] H. Fritzsch and Z. Xing. Phys. Lett. B 372 (1996) 265.
- [19] L. Wolfenstein. Phys. Rev. D17 (1978) 2369; D20 (1979) 2634.
- [20] S. P. Mikheyev and A. Yu. Smirnov. Il Nuovo Cimento C9 (1986) 17.
- [21] V. Barger et al. Phys. Rev. D22 (1980) 2718.
H. A. Bethe. Phys. Rev. Lett. 56 (1986) 1305.
S. P. Rosen and J. M. Gelb. Phys. Rev. D34 (1986) 969.
J. Bouchez et al. Z. Phys. C32 (1986) 499.
- [22] K. Winter. Proc. Beijing Conf. on Lepton Photon interactions (1995).
CERN PPE/95-165.
- [23] D. H. Perkins. Nucl. Astro-Part. Phys. 2 (1994) 1.
- [24] C. R. Proffitt. Ap. J. 425 (1994) 849.
- [25] J. N. Bahcall and M. H. Pinsonneault.
Rev. Mod. Phys. 64 (1992) 885; 67 (1995) 781.
- [26] S. Turk-Chieze et al. Phys. Rep. 230 (1993) 57.
- [27] A. Dar and G. Shaviv. Nucl. Phys. B (proc suppl.) 38 (1995) 235.
- [28] S. T. Petcov. Nucl. Phys. B (Proc. Suppl.) 43 (1995) 12.
- [29] S. L. Glashow and L. M. Krauss. Phys. Lett. B190 (1987) 199.
- [30] P. I. Krastev and S. T. Petcov Phys. Lett. B 299 (1993) 99.
- [31] G. T. Ewan et al. Sudbury Neutrino Observatory Proposal.
SNO-87-12 (1987).
- [32] Y. Totsuka. ICCR-Report 359-96-10 (1996).
- [33] C. Athanassopoulos et al. Phys. Rev. Lett. 75 (1995) 2650; 77 (1996) 3082.

- [34] J. E. Hill. Phys. Rev. Lett. 75 (1995) 2694.
- [35] B. Armbruster et al. Nucl. Phys. B (Proc. Suppl.) 38 (1995) 235.
- [36] B. Blumenfeld et al. Phys. Rev. Lett. 62 (1989) 2237.
- [37] A. Acker and S. Pakvasa. hep-ph/9611423 (1996).
- [38] N. Armenise et al. CERN SPSC/P254.
- [39] P. Astier et al. CERN SPSC/P261.
- [40] Y. Declais et al. CHOOZ proposal (1993).
- [41] F. Boehm et. al. The Palo-Verde Neutrino Oscillation Experiment. (1995).
- [42] E. Ables et al. FNAL Proposal P-875 (1995).
- [43] K. Nishikawa. INS-Rep-924 (1992).
- [44] C. Rubbia. CERN-PPE/93-08.
- [45] P. F. Smith. International Workshop on Identification of Dark Matter. Sheffield (1996).

Figure Captions

Figure 1. The atmospheric neutrino ratio $R = (\mu/e)_{DATA}/(\mu/e)_{MC}$ for contained events from the various underground experiments. The errors plotted combine in quadrature the statistical and systematic errors given in Table 1 and should be largely independent from experiment to experiment. There is no evidence for a discrepancy between the results of the water-Cerenkov and the tracking detectors. The data are consistent with the threefold maximal mixing prediction $R = 2/3$ (broken line).

Figure 2. a) The atmospheric neutrino ratio R plotted versus the flux ratio $F = \phi(\nu_\mu)/\phi(\nu_e)$ for all the data with $L/E > 10^2$ km/GeV. Threefold maximal mixing predicts the dependence shown (dashed curve) while the Fritzsche-Xing ansatz [18] predicts no dependence (dotted line). b) The corresponding χ^2 plotted as a function of $\sin 2\theta \cos 2\phi$ (see text) for a range of ansätze with the tau-lepton maximally-mixed. The Fritzsche-Xing ansatz corresponds to $\sin 2\theta \cos 2\phi = 1$ and is ruled-out by the data, while threefold maximal mixing predicts $\sin 2\theta \cos 2\phi = 0$, which is close to the χ^2 -minimum.

Figure 3. The ratio S of observed to predicted rates in the four existing solar neutrino experiments for each of four solar model predictions. The KAMIOKA and HOMESTAKE values depend principally on the calculated ${}^8\text{B}$ flux and show a wide scatter, while the two gallium experiments are sensitive mainly to pp neutrinos, for which the differences between the models are small. The broken line shows the threefold maximal mixing prediction $P(e \rightarrow e) = 5/9$ which is in excellent agreement with the gallium data. The scenario of Giunti et al. [4] and that of Acker et al. [17] predict $P(e \rightarrow e) \simeq 1/3$ for gallium and are now excluded by the data.

Figure 4. Fits to the solar data plotted as a function of L/E (solid curves). The total ${}^8\text{B}$ flux has been taken as an adjustable parameter in these fits: a) $\Phi({}^8\text{B}) = 3.4 \times 10^6$ $\text{cm}^2 \text{s}^{-1}$; b) $\Phi({}^8\text{B}) = 4.4 \times 10^6$ $\text{cm}^2 \text{s}^{-1}$, $\sin \theta = 0.030$, $\Delta m^2 = 0.61 \times 10^{-5}$ eV^2 ; c) $\Phi({}^8\text{B}) = 6.5 \times 10^6$ $\text{cm}^2 \text{s}^{-1}$, $\sin \theta = 0.50$, $\Delta m^2 = 2.1 \times 10^{-5}$ eV^2 and d) $\Phi({}^8\text{B}) = 2.77 \times 10^6$ $\text{cm}^2 \text{s}^{-1}$, $\sin \theta = 0.71$, $\Delta m^2 = 1.8 \times 10^{-10}$ eV^2 . The data points in each case are calculated using the above flux values (see text). The broken curves show the effect of varying the neutrino mass by a factor of 100 up or down with respect to the best-fit value, with no dependence in threefold maximal mixing ($P(e \rightarrow e) = 5/9$).

Figure 5. The predicted appearance probability $P(l \rightarrow l')$ in the threefold maximal mixing scenario with $\Delta m^2 = 0.72 \times 10^{-2} \text{ eV}^2$ [3]. The LSND result [33] is indicated together with the upper limit obtained by Hill [34] from a subset of the LSND data. Upper limits from KARMEN [35] and BNL-776 [36] are shown, together with the projected sensitivities (90% upper limits, assuming no signal) of the CHORUS [38] and NOMAD [39] experiments.

Figure 6. The predicted event rate spectra in the threefold maximal mixing scenario [3] for a) The CHOOZ [40] and PALO-VERDE [41] reactor experiments and b) the MINOS [42] long-baseline accelerator experiment. Corresponding predictions c) and d) for disappearance and appearance probabilities are also shown, as a function of neutrino energy.

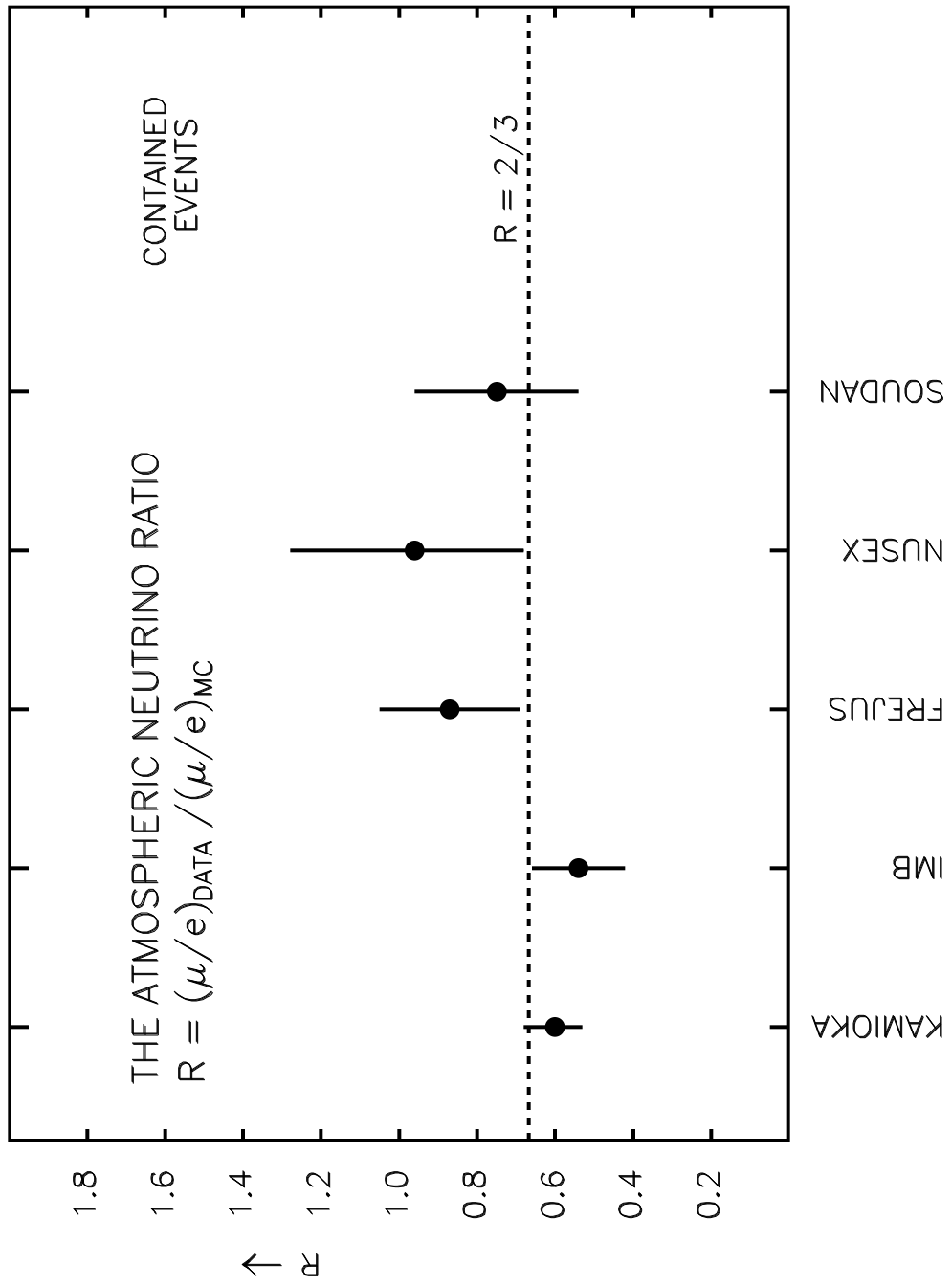


Figure 1

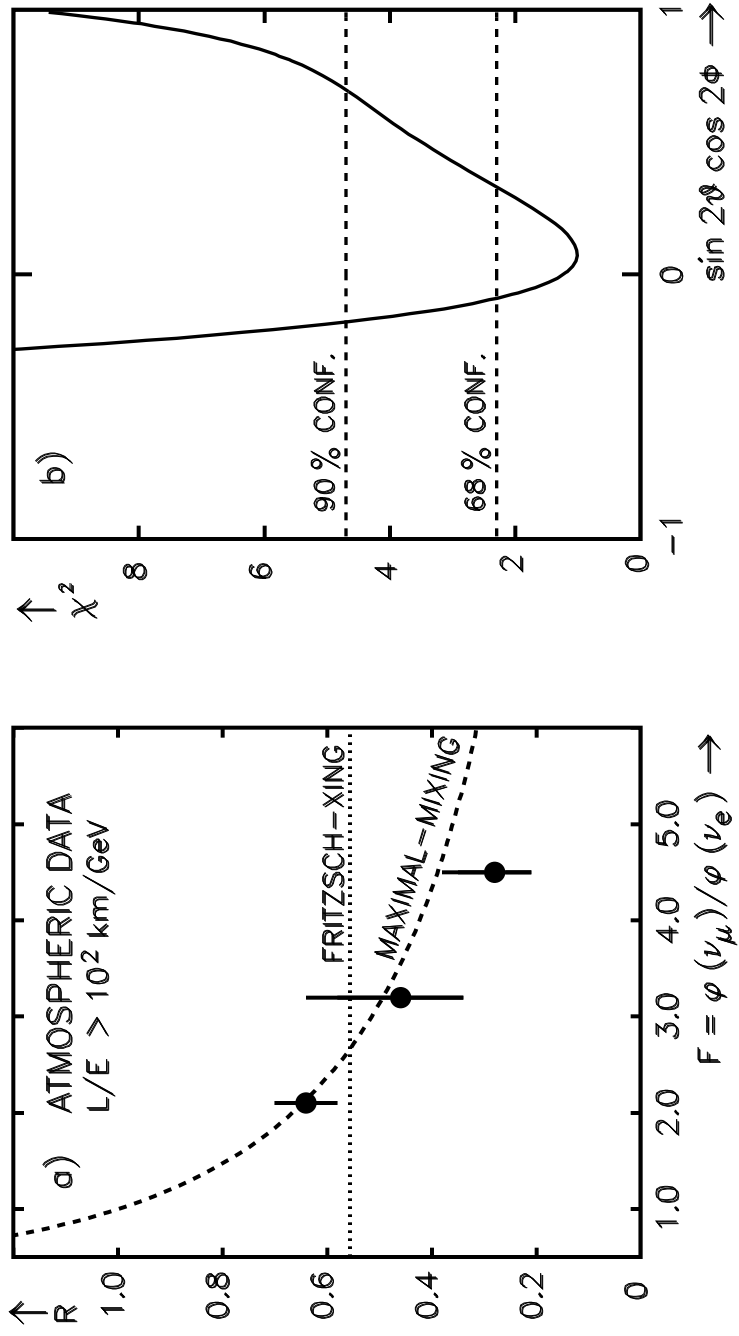


Figure 2

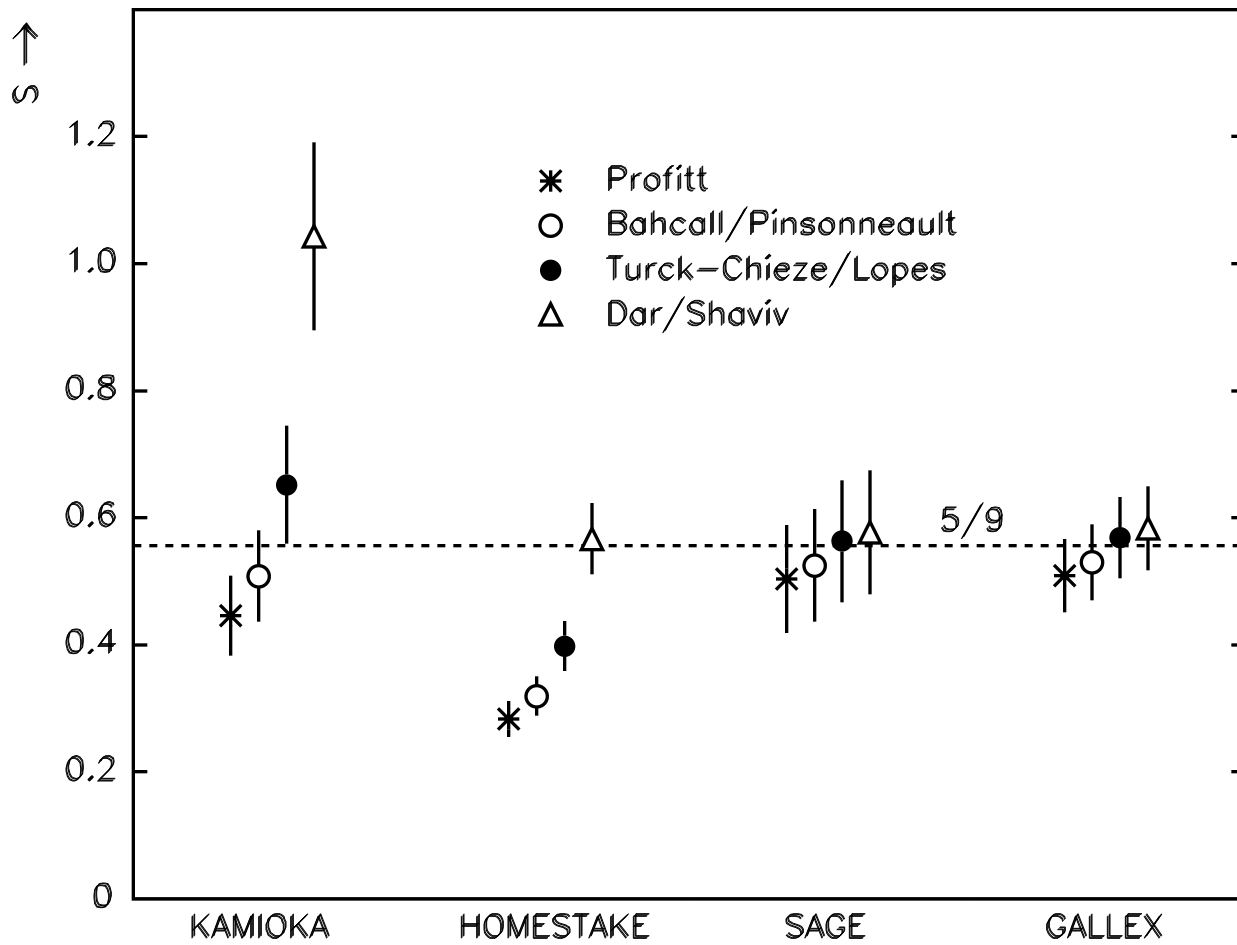


Figure 3

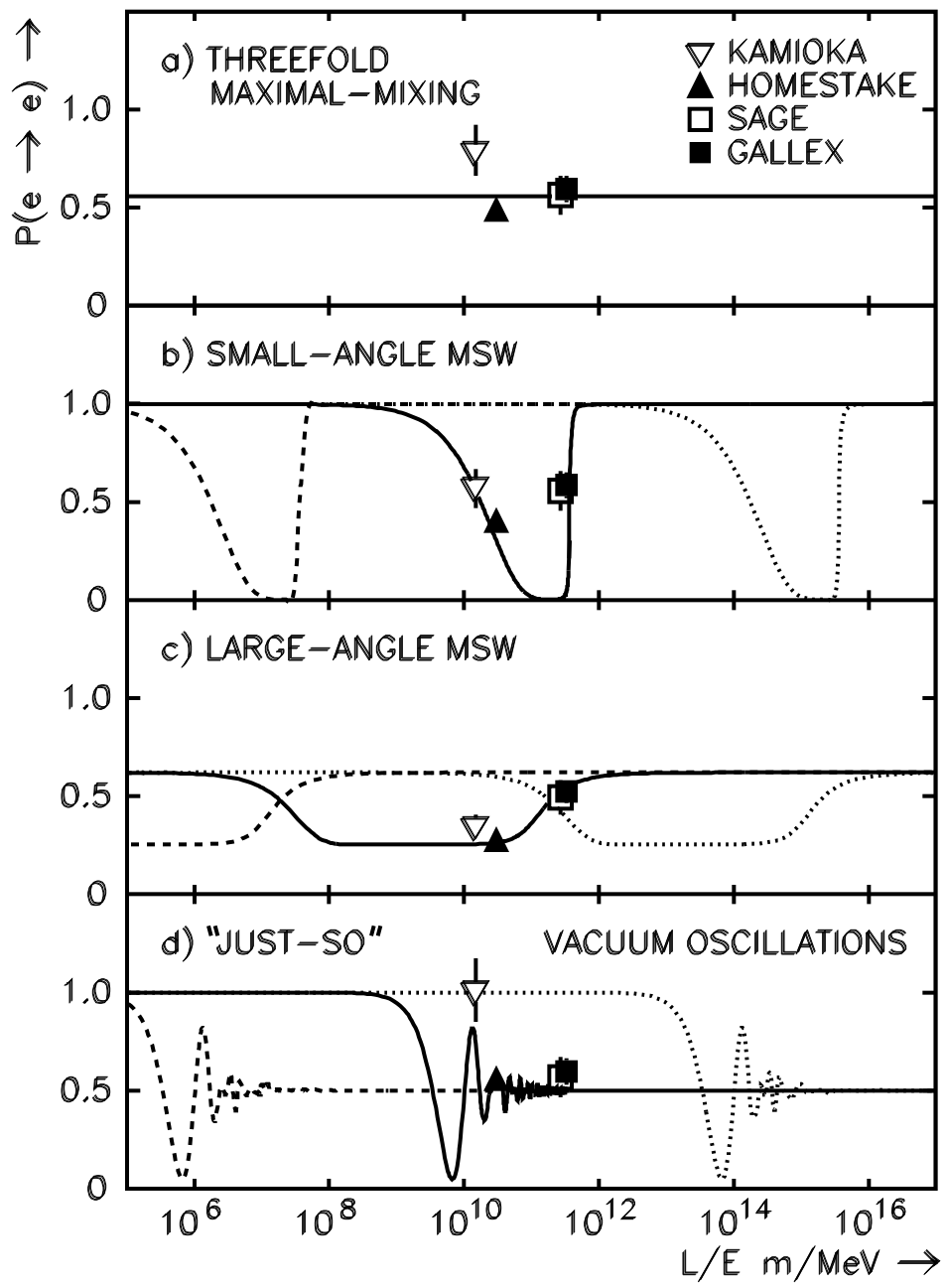


Figure 4

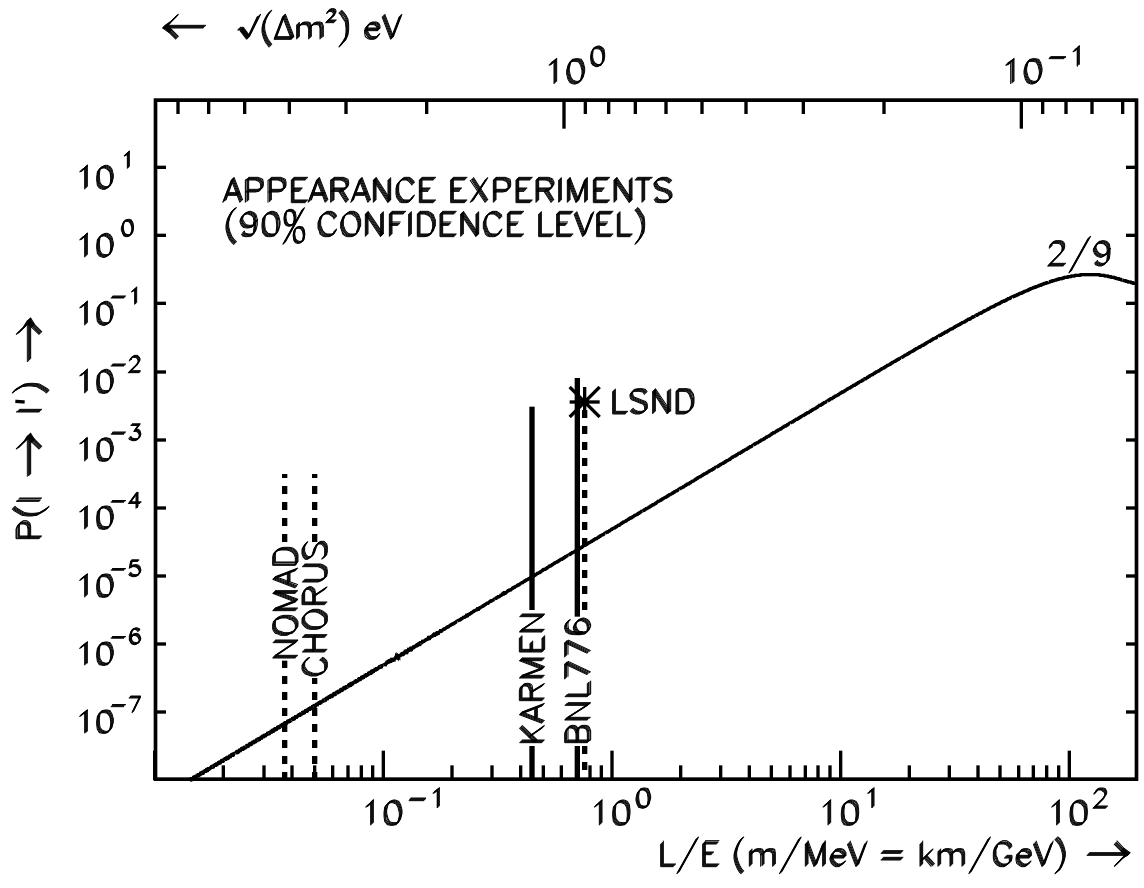


Figure 5

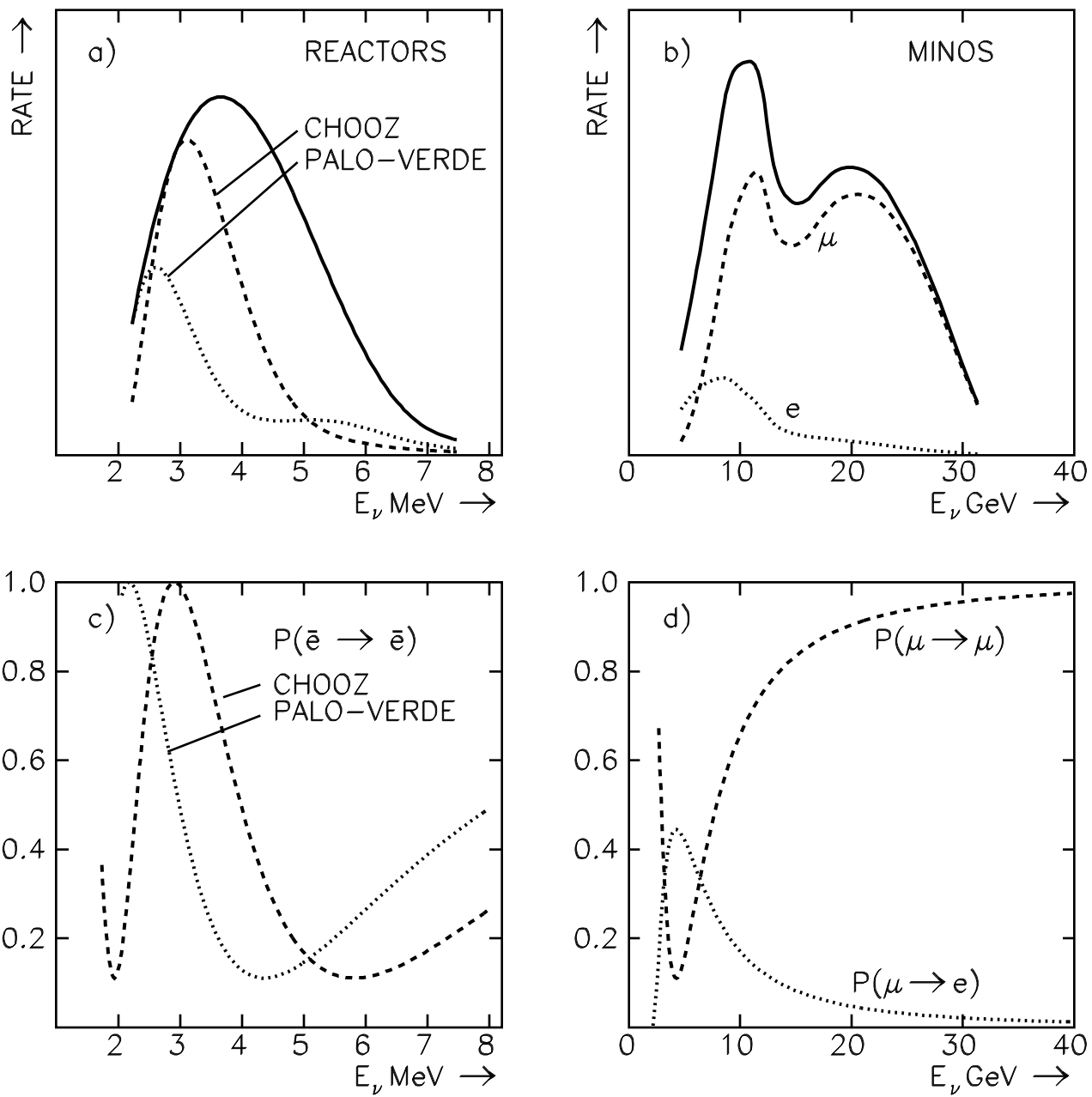


Figure 6

Experiment	kton yr	$R \pm \text{stat.} \pm \text{sys.}$
KAMIOKA	6.1	$0.60 \pm 0.06 \pm 0.05$
IMB	7.7	$0.54 \pm 0.05 \pm 0.11$
FREJUS	1.56	$0.87 \pm 0.16 \pm 0.08$
NUSEX	0.40	$0.96 \pm 0.28 \pm 0.00$
SOUDAN	1.52	$0.72 \pm 0.19 \pm 0.07$

Table 1: The atmospheric neutrino ratio $R = (\mu/e)_{DATA}/(\mu/e)_{MC}$ for contained events, from the various underground experiments. A common $\pm 5\%$ contribution to the systematic error, coming from the uncertainty in the predicted flux ratio, has been subtracted from the quoted systematic error where appropriate. A weighted mean of the above results, adding the statistical and systematic errors in quadrature, yields $R = 0.64 \pm 0.06$, where the common $\pm 5\%$ flux-ratio error is now included.

Experiment (Units)	Meas. \pm stat. \pm sys.	Non- ^8B Flux	^8B Flux	$P(e \rightarrow e)$
KAMIOKA ($10^6 \text{ cm}^{-2} \text{ s}^{-1}$)	$2.80 \pm 0.19 \pm 0.33$	—	3.42 ± 0.36	0.79 ± 0.13
HOMESTAKE (SNU)	$2.55 \pm 0.17 \pm 0.18$	1.58 ± 0.02	3.59 ± 0.38	0.49 ± 0.05
SAGE (SNU)	$69.0 \pm 10.0 \pm 7.0$	112.1 ± 0.3	8.3 ± 0.9	0.57 ± 0.10
GALLEX (SNU)	$69.7 \pm 6.7 \pm 4.5$	112.1 ± 0.3	8.3 ± 0.9	0.58 ± 0.07

Table 2: New results obtained in the context of the threefold maximal mixing scenario by refitting the existing solar neutrino data, assuming $P(e \rightarrow e) = 5/9$, taking the ^8B flux as a free parameter. The non- ^8B fluxes are interpolated linearly between four flux models in the fit, as a function of the ^8B flux. The errors given on the fitted fluxes are (inter-) correlated, while the errors given for $P(e \rightarrow e)$ are just the experimental errors on the individual measurements. In the case of the KAMIOKA result, the value of $P(e \rightarrow e)$ has been corrected for neutral current effects (see Ref. [3]).